This is an open access article published under a Creative Commons Non-Commercial No Derivative Works (CC-BY-NC-ND) Attribution License, which permits copying and redistribution of the article, and creation of adaptations, all for non-commercial purposes.

JACS JOURNAL OF THE AMERICAN CHEMICAL SOCIETY

Article

Cite This: J. Am. Chem. Soc. 2018, 140, 2127−2134

pubs.acs.org/JACS

# Tunable Self-Assembly of $YF_3$ Nanoparticles by Citrate-Mediated Ionic Bridges

Jordi Martínez-Esaín,[†,‡] Jordi Faraudo,[*,‡] Teresa Puig,[‡] Xavier Obradors,[‡] Josep Ros,[†] Susagna Ricart,[‡] and Ramón Yáñez[*,†]

[†]Departament de Química, Universitat Autònoma de Barcelona, 08193 Bellaterra, Spain

[‡]Institut de Ciència de Materials de Barcelona (ICMAB-CSIC), 08193 Bellaterra, Spain

Supporting Information

**ABSTRACT:** Ligand-to-surface interactions are critical factors in surface and interface chemistry to control the mechanisms governing nanostructured colloidal suspensions. In particular, molecules containing carboxylate moieties (such as citrate anions) have been extensively investigated to stabilize metal, metal oxide, and metal fluoride nanoparticles. Using $YF_3$ nanoparticles as a model system, we show here the self-assembly of citrate-stabilized nanostructures (supraparticles) with a size tunable by temperature. Results from several experimental techniques and molecular dynamics simulations show that the self-assembly of nanoparticles into supraparticles is due to ionic bridges between different nanoparticles. These interactions were caused by cations (e.g., ammonium) strongly adsorbed onto the nanoparticle surface that also interact strongly with nonbonded citrate anions, creating ionic bridges in solution between nanoparticles. Experimentally, we observe self-assembly of nanoparticles into supraparticles at 25 and 100 °C. Interestingly, at high temperatures (100 °C), this citrate-bridge self-assembly mechanism is more efficient, giving rise to larger supraparticles. At low temperatures (5 °C), this mechanism is not observed, and nanoparticles remain stable. Molecular dynamics simulations show that the free energy of a single citrate bridge between nanoparticles in solution is much larger than the thermal energy and in fact is much larger than typical adsorption free energies of ions on colloids. Summarizing our experiments and simulations, we identify as key aspects of the self-assembly mechanism the requirement of NPs with a surface able to adsorb anions and cations and the presence of multidentate ions in solution. This indicates that this new ion-mediated self-assembly mechanism is not specific of $YF_3$ and citrate anions, as supported by preliminary experimental results in other systems.

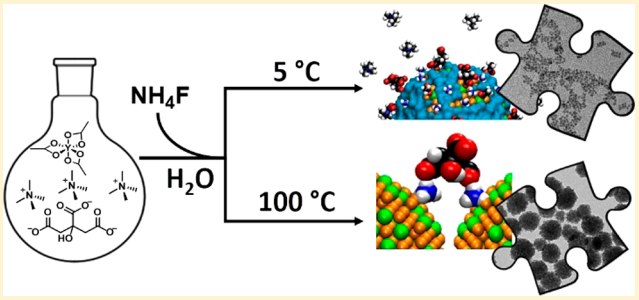


## INTRODUCTION

Nanoscale structures present multiple edge positions, which play a pivotal role on the tailoring and control of their physicochemical properties. However, their characteristic large surface-to-volume ratio entails difficulties on the stabilization and lifetime for characterization and potential applications.[1] Small particles are prone to aggregate as consequence of the intrinsic high thermodynamic energy, reducing the surface-to-volume ratio and hence the surface energy.[2] Surface chemistry plays a significant role in understanding and controlling the nanoparticles' (NPs) aggregation and instability. Coagulation (i) and self-assembly (ii) are the main mechanisms for aggregation of colloidal NPs. The first process (i) involves a noncontrolled growth process,[3] whereas the second proposed route (ii) entails an ordered organization. The high interest in the self-assembly route in recent years is due to its broad possibilities,[4,5] while the uncontrolled coagulation route must be avoided in nanomaterials design.

Here, we propose a new mechanism for the tunable self-assembly of NPs in water media: the formation of an ionic bridge (mediated in particular by citrate) between NPs stabilized by ionic ligands. This mechanism (the appearance of self-assembled supraparticles and their sizes) is found to be controlled by temperature. We think that this new mechanism could be of interest for a wide class of NPs, stabilized by ionic ligands.

Direct ligand coordination is one of the preferred methodologies proposed to control NP-NP interactions and prevent undesired coagulation because of the stability of the bond between the ligand and the NP surface. Recently Owen[6] has discussed ligand-NP bonding in detail, claiming that the ligand-surface interaction can be studied similarly to a classic coordination complex. Using covalent bond classification (CBC),[7] L-, X-, and Z-type ligands can be distinguished considering the number of electrons that the ligand contributes to surface bonds onto the NP surface. L-type are Lewis bases with two-donor electrons, X-type are single-electron donors in their neutral form, and Z-type are Lewis acids with zero-donor electrons. Among the different options for the ligands, polydentate carboxylate ligands are excellent candidates, stabilizing the surface of NPs by direct carboxylic-to-metal

Received: September 14, 2017
Published: January 8, 2018


© 2018 American Chemical Society

DOI: 10.1021/jacs.7b09821
J. Am. Chem. Soc. 2018, 140, 2127−2134

coordination. Citrate stabilization is one of the most efficient routes.[6−8] In fact, biomedical applications based on citrate-stabilized NPs are of interest for their biocompatibility and their high water stability.[9,10] For this reason, we considered here citrate-stabilized NPs.

For the NP, we decided to use $YF_3$ as a model system. The reason is that potential applications of lanthanide fluoride NPs are currently under study in a variety of medical fields: photodynamic therapy,[11,12] positron emission tomography (PET) imaging using $^{18}F$ as radionuclei,[13] contrast agents by up/down-conversion fluorescence properties,[14,15] and magnetic resonance imaging (MRI).[16] Their low solubility in water and their biocompatible functionalization of the surface make them suitable for studies on cancer therapy.[17,18]

NP surfaces with coordinated ligands are complex systems, and their study requires the use of multiple techniques.[19−21] A combination of experimental characterization and molecular dynamics (MD) simulation methodologies makes a detailed investigation of NP interfaces possible and useful for a rational design in biological applications.[22,23]

Additionally, here this dual approximation will provide us information on the surface at atomic level useful to understand general self-assembly mechanisms.[24−27]

## RESULTS AND DISCUSSION

**Particle Synthesis and Characterization.** Citrate-stabilized $YF_3$ particles were successfully synthesized using a modified co-precipitation method[13] (see Methods section to more details). Yttrium(III) acetate and tetramethylammonium citrate were dissolved in water (sodium cation was avoided to prevent the competitive effect[28] between $NaYF_4$ and $YF_3$). We employed an Y:Citrate molar ratio of 1:1.5. This molar ratio was chosen due to the insolubility of yttrium citrate at molar ratios below this one.[29] Then, when a specific temperature was achieved (100 or 5 °C depending on the case), ammonium fluoride was injected dropwise to start the nucleation process for a reaction time of 2 h.

Using a reaction temperature of 5 °C, we obtain monodisperse $YF_3$ NPs, as shown in Figure 1a by transmission electron microscopy (TEM) and dynamic light scattering (DLS). DLS gives a narrow particle size distribution, centered at a volume averaged hydrodynamic diameter of 7.5 nm (Figure 1a). According to TEM, NPs have an average diameter of 5 nm (see TEM histogram in Figure S1). X-ray diffraction (XRD) characterization of synthesized NPs (see Figure S1) is compatible with a cubic crystalline structure. Using our XRD data in Scherrer equation,[30] we obtain a crystalline coherent domain of 4.4 nm, in agreement with the NP size determined by TEM.

When the reaction is carried out at 100 °C, we unexpectedly found that the result of the synthesis consists of supraparticles formed by self-assembly of small NPs. The spherical assemblies have a narrow size distribution with a peak at ∼80 nm (Figure 1b). They have a crystal structure compatible with the cubic phase characteristic of $YF_3$ (Figure S2). Using the XRD pattern obtained from these supraparticles and applying the Scherrer equation, a crystal coherent domain of 6.5 nm was obtained. TEM and XRD characterization confirmed the presence of supraparticles formed by smaller monocrystalline NPs. According to our electrokinetic measurements (see Table S1), both NPs at 5 °C and supraparticles at 100 °C are negatively charged with values of $\xi$-potential that ensure colloidal stability in water ($\xi$-potential ≈ −40 mV).

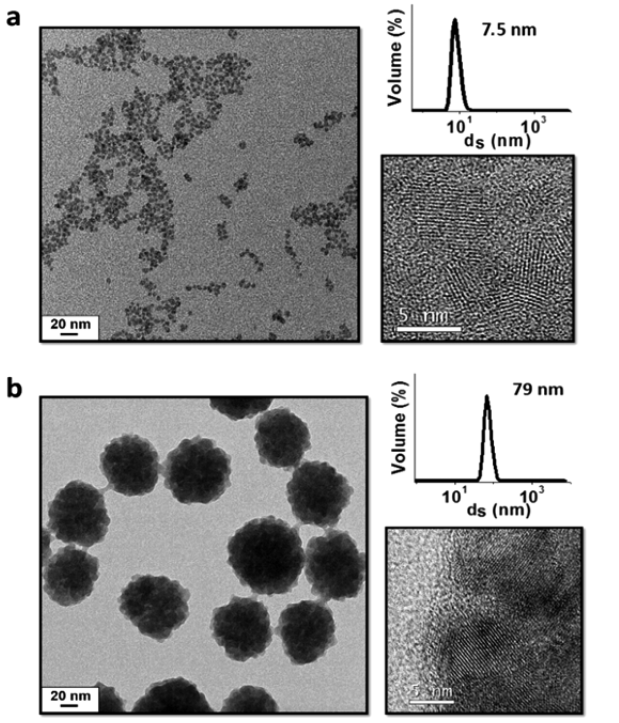


**Figure 1.** Particle size DLS measurements (% in volume) with the corresponding TEM and HRTEM micrographs of as-synthesized nano/supraparticles at 5 °C (a) and at 100 °C (b).

**Tuning the Size of Supraparticles.** The final size of the supraparticles made by self-assembly of NPs could be controlled by two key factors: (i) the temperature and (ii) the specific ions present at the surface of the colloidal system.

Synthesis at 25 °C was performed to demonstrate the effect of temperature (Figure S3). Smaller supraparticles of ∼40 nm were obtained in this case (compare with ∼80 nm of those obtained at 100 °C), thus demonstrating the dependence of the supraparticles size with temperature. XRD measurements and Scherrer equation give, for this case, a crystalline coherent domain of 5.1 nm. This value is intermediate between the ones obtained at 5 and 100 °C (4.4 and 6.5 nm, respectively).

In order to demonstrate the role of specific ions in the self-assembly process, we have considered several different cations or anions as precursors for the synthesis process performed at 100 °C. First, we have tested the effect of considering a bigger cation by using tetrabutylammonium fluoride instead of ammonium fluoride. In this case, we obtained bigger $YF_3$ supraparticles of 179 nm (Figure S4), formed by the assembly of NPs of 3.8 nm size as determined by Scherrer equation (Table S2). Note that these supraparticles have a diameter about two times larger than the ones obtained using ammonium fluoride. This demonstrates that the cation plays a substantial role in the self-assembly process of NPs into supraparticles.

We have also considered several options for the metal precursor. At 100 °C, we have replaced yttrium(III) acetate by yttrium(III) trifluoroacetate, chloride, and nitrate. In all three cases (see Figure S5), we obtained very similar supraparticles with a size of ∼100 nm as measured by DLS, larger than the 80 nm supraparticles obtained with yttrium(III) acetate. We interpret this experimental result as an indication that the anions do not play a significant role in the self-assembly process


DOI: 10.1021/jacs.7b09821
J. Am. Chem. Soc. 2018, 140, 2127−2134

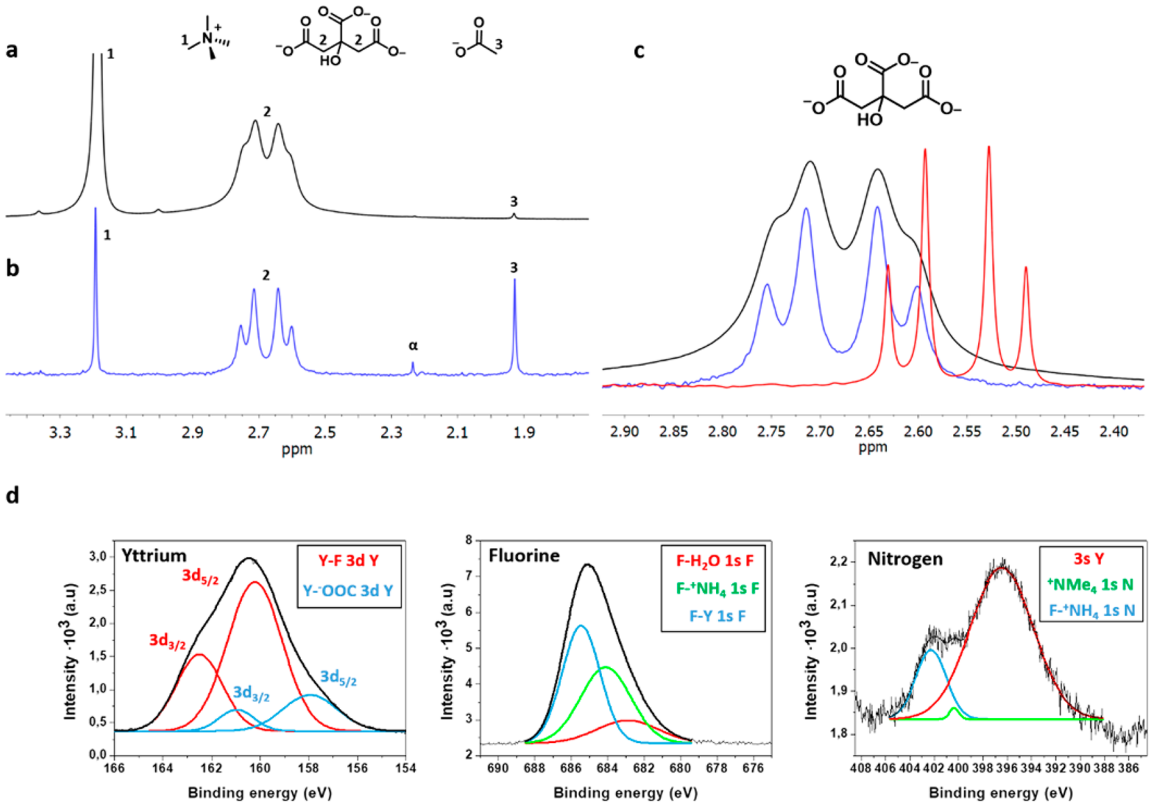


**Figure 2.** $^1$H NMR of $YF_3$ NPs synthesized at 5 °C (a) and $YF_3$ supraparticles synthesized at 100 °C (b). The assignments of the peaks (black numbers) corresponding to the ions present in the system for both cases (5 and 100 °C) are indicated in the chemical structures for an easier interpretation. The peak indicated with $\alpha$ corresponds to nonsolvent impurity. (c) Comparison of citrate signal of $YF_3$ NPs synthesized at 5 °C (black), $YF_3$ supraparticles synthesized at 100 °C (blue) and free citrate (red). (d) XPS of $YF_3$ supraparticles synthesized at 100 °C. Deconvoluted regions of XPS with their corresponding assignation to each Gaussian function of: yttrium (left), fluorine (middle) and nitrogen (right). $^1$H NMR and XPS measurements were carried out with a sample washed five times. All peaks were deconvoluted using the minimum number of Gaussian functions necessary to obtain the same signal.

of NPs into supraparticles. It also indicates that acetate stabilizes better the NPs surface than the other anions.

The combined effect of temperature and the presence of free ions in solution is also critical for the formation of supraparticles. This is demonstrated by the following experiments. First, unwashed NPs synthesized at 5 °C are heated to 100 °C for 2 h. We observe the formation of supraparticles with a size of ∼40 nm following a controlled aggregation process (Figure S6). In the second experiment, NPs synthesized at 5 °C were washed thoroughly before heating to 100 °C (see Scheme S1 for details). In this case, the NPs dispersion remains unaltered, and no supraparticles were formed (Figure S7).

Therefore, our experimental results show that the availability of free ions in solution is essential for the observed self-assembly of NPs into supraparticles and that the self-assembly process is controlled by temperature. This suggests that the self-assembly mechanism is mediated by the interaction of free ions with the surface of the NPs when thermal energy increases above certain activation energy. The identification of the self-assembly mechanism thus requires a detailed investigation of the interaction of the ions with the interface.

**Interface Characterization.** In order to understand the observed effect of ions, we have investigated their interaction with the surface of the $YF_3$ particles by employing $^1$H NMR, IR, and XPS.

The results of $^1$H NMR show the presence of citrate and tetramethylammonium at 5 °C (Figure 2a), while at 100 °C, we observe the presence of citrate, acetate, and tetramethylammonium (Figure 2b). Note that to ensure a clear identification of adsorbed species, $YF_3$ particles were washed five times to avoid overlapping signals from free ions. Comparison of the signals obtained in Figure 2a,b with that expected for free citrate are shown in Figure 2c. Free citrate signal is found at a higher field and is narrower. The displacement of the citrate signal to lower field in Figures 2a,b is due to the interaction of the carboxylic moiety of citrate with yttrium atoms of the NP.

We interpret the different broadness of the signals for adsorbed citrate at 5 and 100 °C as corresponding to two different binding modes of citrate with the NP surface. We propose that each adsorbed citrate is coordinated preferentially with yttrium atoms of the surface by one carboxylic moiety at 5 °C and by two carboxylic groups at 100 °C (see more details in the Supporting Information and in Figure S10).

IR spectroscopy characterization was performed to complement our NMR study (Figure S9 and Table S4). We observed bands at 1581 and 1421 $cm^{-1}$ at 5 °C and 1588 $cm^{-1}$ and ∼1423 $cm^{-1}$ at 100 °C. In both cases, these bands correspond to symmetric and asymmetric stretching of carboxylates, and the difference between them of ∼160 $cm^{-1}$ is compatible with an ionic interaction of carboxylate moieties of citrate with $YF_3$ NP (see details in the Supporting Information).

Concerning XPS characterization, the results are shown in Figure 2d and Figure S11. In the case of yttrium, we have two peaks: $3d_{5/2}$ at 160 eV corresponding to the interaction with


DOI: 10.1021/jacs.7b09821
J. Am. Chem. Soc. 2018, 140, 2127−2134

fluorine in $YF_3$ and $3d_{5/2}$ at 158 eV corresponding to the Y-OOC- interaction.[31] Concerning the latter broad peak, we consider that this peak encompasses acetate, citrate, and water (all Y-O interactions). In the case of fluorine spectra, it shows three different peaks: $YF_3$ at 686 eV,[32] F-$^+NH_4$ at 684 eV and a broad peak of F−$H_2O$ at 683 eV, produced by solvation water directly attached to the surface of the NPs. Finally, the results for the nitrogen region are compatible with the presence of two different species: one as counterion (tetramethylammonium cations) and the other (ammonium cations) attached directly onto NPs surface at higher binding energy. The largest peak observed at this region corresponds to the 3s Y signal,[33] which overlaps with the nitrogen signals, interfering with the direct assignment.

Therefore, the results from the surface characterization show that the obtained particles have adsorbed citrate and acetate anions coordinated with yttrium atoms of the surface and ammonium cations coordinated with fluorine atoms of the surface. The presence of these adsorbed ions over the surface is expected to play a decisive role in the interactions between particles in the self-assembly process between them. Also, we have seen in our experiments that the presence of free ions in solution is necessary for the observed self-assembly of NPs into supraparticles. To identify the atomistic mechanism of the self-assembly process and the role of each factor (adsorbed ions, free ions and temperature), we decided to perform atomistic MD simulations.

**Image of the NP/Solution Interphase by MD Simulations.** We first performed large-scale all-atomic MD simulations[34] of an electrically neutral $YF_3$ NP in solution at both 5 and 100 °C. To achieve a realistic simulation, we consider in our simulation system a full atomistic description of a NP in a solution containing explicit water molecules and free ions (see detailed description in the Supporting Information). The use of MD simulations in solution with atomistic detail requires the use of substantial computational resources, but it has many advantages as compared with other commonly employed techniques,[20,35] since it allows to obtain the spontaneous evolution of the system (e.g., obtain equilibrium adsorption of ions from an initial state without adsorbed ions) at the relevant temperature and pressure. MD simulations give crucial information about the affinity of the species with the colloidal surface as well as the binding motif onto this surface.

Our MD simulations (Figure 3) predict that at 5 °C the surface of an $YF_3$ NP is spontaneously covered by irreversibly adsorbed acetate, citrate, and ammonium ions, while tetramethylammonium cations are not adsorbed onto the surface. Our MD simulations also predict that at 5 °C, a neutral $YF_3$ particle will be negatively charged due to ion adsorption, since the negative charge from adsorption of citrate and acetate is larger than the charge from the adsorbed ammonium (see Table S7). This result is consistent with the negative charge inferred from electrokinetic experimental results. Simulation performed at 100 °C shows that an $YF_3$ NP will also adsorb acetate, citrate, and ammonium ions (with an excess of anionic over cationic charge), although larger amounts of adsorbed ions than those obtained at 5 °C are observed (Table S7). These results also provide clear examples of X-type (bound ion pair) stabilization[36] onto NP surface. One ion pair is formed by acetate and ammonium directly attached onto NP surface. Citrate is also forming an ion pair system, neutralized with ammonium in the Stern layer and tetramethylammonium in the diffuse double layer.

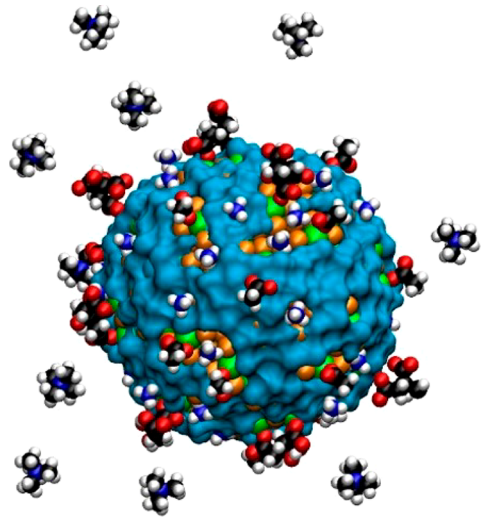

**Figure 3.** Snapshot (made with VMD)[37] from MD simulations at 5 °C showing adsorbed citrate, acetate, and ammonium ions in van der Waals representation. Also, we show tetramethylammonium counter-ions diffusing close to the NPs. Green and orange spheres correspond to yttrium cations and fluoride anions, respectively. The molecular surface (made using the surface algorithm of VMD) defined by adsorbed water is shown in blue. Water molecules are not shown for clarity.

Electrostatic interactions are responsible for the high affinity of these ions to the surface, but we also expect that solvation water plays a significant role, preventing the adsorption of tetramethylammonium. We have tested this hypothesis by performing additional MD simulations in a primitive model (i.e., replacing explicit water molecules by a dielectric medium with $\varepsilon = 80$). In these cases, there were a massive condensation of tetramethylammonium ions at both temperatures (see Supporting Information for details).

Our MD simulations also show that at 5 and 100 °C most of the adsorbed citrate ions (62% at 5 °C and 70% at 100 °C, see Supporting Information) are coordinated with two yttrium atoms employing two carboxylic groups. The remaining adsorbed citrates are attached to a single yttrium with one carboxylic group. Interestingly, NMR results suggest that the fraction of strongly adsorbed citrate ions (those that remain adsorbed after the washing process) is significantly higher at 100 °C than at 5 °C.

**Unravelling the Self-Assembly Mechanism.** To study the interaction between the surfaces of two $YF_3$ NPs close to contact, we performed further simulations described in detail in the Supporting Information. These simulations were designed to describe NPs interacting at different distances. The simulation describing NPs interacting at a distance of ∼7 Å showed crucial information on the self-assembly mechanism. At 100 °C, we observed the formation of ionic bridges between two $YF_3$ surfaces, as seen in Figure 4a. These bridges were formed spontaneously by a citrate anion interacting with two adsorbed ammonium cations, as seen in Movie S1. Each ammonium cation is adsorbed onto a different $YF_3$ particle, and a citrate is forming a bridge using different carboxylates for each ammonium. The spontaneous formation of citrate bridges is not observed in simulations at 5 °C.

We have also performed adaptive biasing force-molecular dynamics (ABF-MD) free energy calculations[38] in order to assess the stability of a citrate bridge at 100 °C. Our simulations



DOI: 10.1021/jacs.7b09821
J. Am. Chem. Soc. 2018, 140, 2127−2134

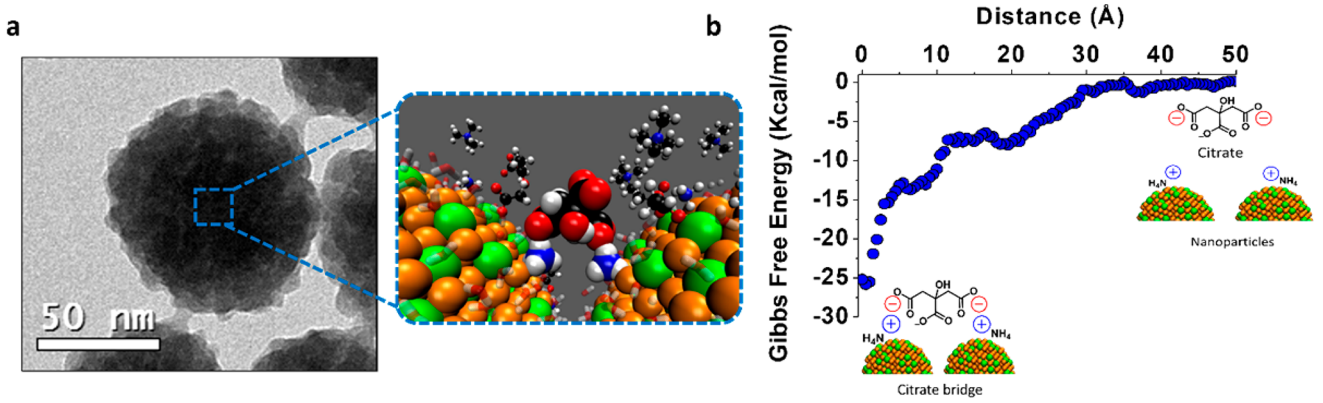


**Figure 4.** (a) TEM image of a single supraparticle obtained at 100 °C (left). We also show (right) a snapshot of our MD simulations at 100 °C in which we obtain a self-assembled citrate bridge between two $YF_3$ surfaces. The two adsorbed ammonium ions linked by the same citrate are shown in van der Waals representation; other ions in the system are shown in CPQ representation. Adsorbed water molecules are also shown. We propose these bridges as the linker of small NPs to form the bigger self-assembled supraparticles. (b) Gibbs free energy (obtained as a potential of mean force in ABF-MD simulations) associated with a single citrate self-assembled cleavage at 100 °C.

predict a free energy per bridge of $\Delta G$ = 25 kcal/mol (~40 times the thermal energy $k_BT$) (Figure 4b). This is a large value for the adsorption free energy of a single ion, indicating that in this system a citrate bridge is highly stable. For comparison, let us recall that typical free energies of adsorption of ions with high affinities for a colloid are of the order of $10k_BT$ (see ref 39). We recall here that these highly stable citrate bridges are obtained only in our MD simulations at 100 °C and are not obtained in MD simulations at 5 °C, a result that is consistent with the experimental observation that supraparticles are formed at 100 °C but are not observed at 5 °C.

Thus, we propose that the mechanism driving the self-assembly of $YF_3$ NPs into supraparticles is the formation of citrate bridges between NPs (Figure 4). The required citrate ions came from ions free in solution, as shown in our MD simulations. This justifies the experimental observation (discussed before in detail) on the key effect of washing the NP solutions to remove free ions.

The formation of these citrate bridges is triggered by the high ionic adsorption of cations onto the surface of the particles, as shown in our MD simulations. Considering the high affinity of ammonium cations to fluoride onto the NP surface (~1.4 ions/nm$^2$ as obtained in MD simulations at 100 °C, corresponding to ~200 adsorbed ammonium ions for a NP of 7 nm size), we expect the formation of citrate bridges between several NPs. Also, since the adsorbed ammonium cations are homogeneously distributed along the spherical NP surface, we can expect the formation of bridges in all directions which will give rise to spherical supraparticles. A multidentate anion (e.g., citrate) is the key molecule needed to produce this bridge interaction with adsorbed cations. The role of the adsorbed ammonium cation also involved in this bridge can be played by other cations. As we have discussed in the Methods section (see also the Supporting Information), a change in the cation employed in the synthesis affects the particles size, but the formation of supraparticles is still observed.

**Presence of the Self-Assembly Mechanism in Other Systems.** Summarizing the experimental and simulation results obtained so far, we see that the mechanism proposed here for a tunable self-assembly of NPs is in fact generic, that is, it is not requiring any specific properties of the particular material used here as a model system ($YF_3$) but only very generic features. Essentially, it requires NPs with a surface able to adsorb anions and cations and the presence of multidentate ions in solution (such as citrate ions) which can create bridges between the NPs covered by absorbed ions.

In order to test this conclusion, we have performed preliminary experiments in different systems, considering different materials for the NPs and/or different multidentate ions. We first considered NPs from materials with different crystalline structures: $SmF_3$ (hexagonal), $EuF_3$ (orthorhombic), and $LuF_3$ (cubic). In all of these cases we obtain NPs at 5 °C and supraparticles at 100 °C, as we observed in $YF_3$. As an example, we show the obtained TEM images for $SmF_3$ in Figure 5a. TEM images and XRD patterns for the NPs (5 °C) and supraparticles (100 °C) obtained with $SmF_3$, $EuF_3$, and $LuF_3$ are also shown in Figure S14 (more extensive analysis for these and other systems will be reported in a forthcoming publication[40]).

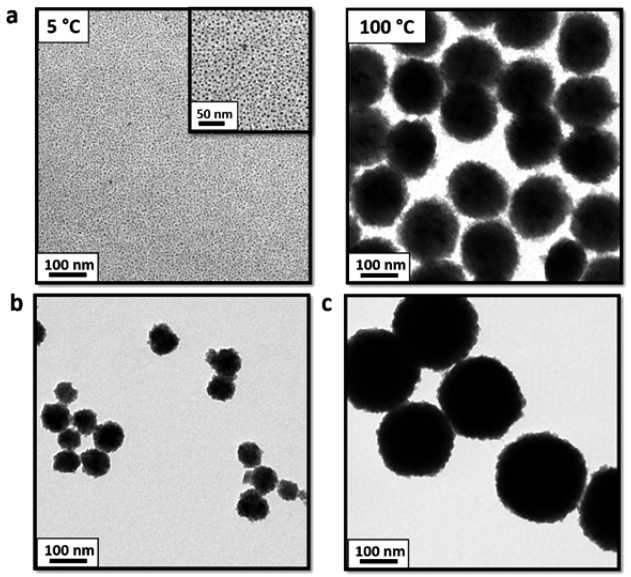


**Figure 5.** (a) TEM images of as-synthesized $SmF_3$ NPs at 5 °C (left) and supraparticles at 100 °C (right). (b) TEM image of $YF_3$ supraparticles obtained at 100 °C using citraconic acid instead of citric acid. (c) TEM image of $YF_3$ supraparticles obtained at 100 °C using maleic acid instead of citric acid.



DOI: 10.1021/jacs.7b09821
J. Am. Chem. Soc. 2018, 140, 2127−2134

After this study with different NPs, we considered again the $YF_3$ case but now we used different multidentate carboxylic ligands to show that the ionic-mediated bridge is not exclusive of citrate anions. Using citraconic acid and maleic acid, we observe the formation of $YF_3$ supraparticles of different sizes at 100 °C (Figure 5) due to the formation of multidentate ionic interactions with adsorbed ammonium cations. The size of the supraparticles depends on the particular multidentate anion employed, as observed in our previous study of the effect of the employed cation (see Tuning the Size of Supraparticles subsection). We obtained $YF_3$ supraparticles of ∼75 nm using citraconic acid (Figure 5b) and bigger ones of ∼200 nm with maleic acid (Figure 5c).

## CONCLUSIONS

Using $YF_3$ as a model system, we propose here a mechanism for the self-assembly of NPs into colloidally stable supraparticles with a tunable size depending on temperature or/and ionic media. The mechanism is based on the formation of a citrate bridge between two different NPs, involving the cooperative interaction of free citrate ions with adsorbed cations onto the NP surface. We have proved that the self-assembled citrate bridge is governed by two key factors: (i) temperature and (ii) the particular cations adsorbed onto the surface of NPs.

Temperature controls the supraparticles formation as well as the size of the final NPs. In our $YF_3$ system at 5 °C, we do not have formation of supraparticles in our experiments, and citrate bridges are not observed in our simulations. At 25 °C, we observe formation of stable supraparticles and at higher temperatures (100 °C). This citrate-bridge self-assembly mechanism is more efficient, giving rise to larger supraparticles. According to our free energy calculation, the value for a single citrate self-assembled bridge ($\sim 40 k_B T$ at 100 °C) is large enough to highlight it as one of the strongest ionic interactions described for colloidal systems in solution.

Concerning factor (ii) (the role of particular cations), it is important to recall that the effect produced by the adsorbed ions is not only related with (electrostatic) stabilization but also plays a pivotal role in the self-assembly process. As shown experimentally and by MD simulations, our $YF_3$ NPs are covered by adsorbed cations and anions (with an excess of adsorbed anions). The adsorbed cations of different NPs interact with citrate ions in solution to form citrate bridges between NPs. As we have seen experimentally, changing the particular cation employed (e.g., using tetrabutylammonium instead of ammonium) results in supraparticles of different size.

Water and solvation effects also play a less obvious but essential role in the self-assembly process. According to our MD simulations, solvation water molecules act as stabilizer avoiding the massive ionic condensation of both cations and anions onto the NPs surface.

The self-assembly mechanism described in this paper does not depend on the particular details of the $YF_3$ system, but rather on very generic features. Essentially, it requires NPs with a surface able to adsorb anions and cations, and it also requires the presence of multidentate ions in solution (as the ubiquitous citrate ions).

The mechanism described here is reminiscent of, but different from, other self-assembly mechanisms described in supramolecular self-assembly, such as ionic self-assembly or ionic bridges. In the case of ionic self-assembly,[41,42] although ions play an important role, the essence of the method is not based on ions. In this case, the method is based on using building blocks of different charge and different chemical properties. In the case of ionic bridges, usually one has typically a multivalent ion that binds simultaneously to two chemical groups, but each one belonging to a different molecule. For example, divalent ions such as $Ca^{2+}$ are able to bind to anionic groups in biomolecules such as lipids or DNA and induce a variety of self-assembled structures.[43,44] The process described here is different in the sense that it involves simultaneously several ionic species (cations adsorbed at the NP surface and free multidentate citrate anions) and it involves different length scales (it involves the self-assembly of NPs in a supraparticle instead of the self-assembly of molecules into a supramolecular structure). The self-assembly of NPs by citrate bridges can be considered a generic mechanism for the self-assembly of inorganic NPs, different than the mechanisms usually considered for the self-assembly of inorganic NPs (see for a review ref 45). In order to test the generality of the mechanism, we also reported here preliminary results in which we observe also the described self-assembly mechanism with other NPs (different of $YF_3$) and other multidentate ions (different from citrate). We expect to report further examples of the use of the present technique in a variety of NP systems in the near future.[40]

## METHODS

**Materials.** Yttrium(III) acetate hydrate 99.9%, yttrium(III) trifluoroacetate 99%, yttrium(III) nitrate hexahydrate 99.8%, yttrium(III) chloride hexahydrate 99.99%, samarium(III) acetate hydrate 99.9%, europium(III) acetate hydrate 99.9%, lutetium(III) acetate hydrate 99.9%, citric acid 99%, maleic acid ≥99%, citraconic acid 98%, tetramethylammonium hydroxide 25% v/v in water, tetrabutylammonium fluoride hydrate 98%, and ammonium fluoride >99.99% were purchased from Sigma-Aldrich. Ethanol 96% from Panreac, acetone 99.5% from Scharlau, and deuterium oxide 99.90% D were purchased from euriso-top. All reagents were used as received without further purification.

**Particle Synthesis.** In a 50 mL round-bottom flask equipped with a condenser and a magnetic stirrer, citric acid (2.25 mmol) in 16 mL of Milli-Q water was neutralized with tetramethylammonium hydroxide (6.75 mmol), followed by the addition of $Y(CH_3COO)_3 \cdot H_2O$ (1.5 mmol). The initial solution was heated until 100 °C or cooled down to 5 °C, and then $NH_4F$ (4.5 mmol) in 4 mL of Milli-Q water was injected dropwise. After 2 h of reaction, the final mixture was allowed to reach room temperature. $YF_3$ particles were separated from the reaction media by the addition of 10 mL of ethanol (supraparticles) or acetone (NPs), followed by centrifugation at 10,000 rpm for 20 min. Separated NPs were redispersed in 20 mL of Milli-Q water, forming a stable dispersion of ∼30 mM.

**Characterization.** DLS and electrophoresis ($\zeta$-potential) analyses have been carried out in Characterization of Soft-Materials Services at ICMAB using a Zetasizer Nano Zs with measurement range of 0.3 nm to 10.0 $\mu$m and sensitivity of 0.1 mg/mL. XRD patterns of the samples were recorded using a Phillips XPert diffractometer equipped with a two circle diffractometers and Cu tube. TEM micrographs were obtained on a 120 kV JEOL 1210 TEM, which has a resolution point of 3.2 Å. High-resolution transmission electron microscopy (HRTEM) micrographs were obtained on a 200 kV JEOL 2011 TEM, which has a resolution point of 1.8 Å at 200 kV. Samples for TEM analysis were prepared by spreading a drop of as-prepared NPs diluted dispersion on amorphous carbon-coated grids and then dried in air. NMR analyses were recorded with a Bruker Advance II 400 spectrometer in $D_2O$ at 298 K. Samples for NMR were prepared washing the colloidal solution five times before drying NPs. Finally, the powder was dispersed in $D_2O$. Infrared spectroscopy (IR) analyses have been carried out in the Servei d'Anàlisi Química with the Bruker spectrophotometer IR Tensor 27. XPS measurements were performed with a Phoibos 150 analyzer (SPECS GmbH, Berlin, Germany) in ultrahigh-vacuum


DOI: 10.1021/jacs.7b09821
J. Am. Chem. Soc. 2018, 140, 2127−2134

conditions (base pressure $4 \times 10^{-10}$ mbar) with a monochromatic aluminum $K_\alpha$ X-ray source (1486.74 eV). The energy resolution as measured by the fwhm of the Ag $3d_{5/2}$ peak for a sputtered silver foil was 0.62 eV.

**Computer Simulations.** All chemical species were described with full atomistic detail. The species included in the simulations are an $YF_3$ NP, four ionic species (citrate, acetate, ammonium and tetramethylammonium), and water. The force field employed for the molecules was the standard CHARMM force field.[46−48] In this force field, interatomic nonbonding interactions are given by electrostatic and Lennard-Jones 12-6 potentials. Bonded interactions in molecules include harmonic bonds, harmonic angle, and dihedral potentials. The molecular models and values of the parameters employed for citrate, acetate, ammonium, and tetramethylammonium are the standard in CHARMM. For water, we employed the TIP3P water model with CHARMM parameters. The modeling of an $YF_3$ NP in a way consistent with the CHARMM force field was done as follows. First, we start building the atomic coordinates of a NP based on the experimental crystallographic information. The experimental X-ray diffraction pattern was compared with standard (04-007-2483) reference of the International Centre for Diffraction Data. Once the structure was verified, the unit cell was obtained using the software Eje-Z.[49] Using this unit cell, we employed the program Rhodius[50] to generate the atomic coordinates of Y and F for $YF_3$ bulk material, which was cut to obtain a spherical NP. We decided to consider a particle of 3 nm diameter, since larger particles will need the use of extremely large simulation boxes in order to also include ions and water. The obtained 3 nm particle had 240 sites for yttrium atoms and 922 sites for fluorine atoms, which does not have the correct 3:1 ratio (occupation factor for F in the pattern = 0.75). In order to correct this structure and obtain a 3:1 ratio, we assumed an occupation number of 1 for yttrium and an occupation number for fluorine sites given by $240 \times 3/922 \approx 0.780911$. Therefore, in the simulations, we fill all sites, and we assigned a partial charge of +3e to the yttrium atoms and a partial charge of −0.780911e to the fluorine atoms. The model of the NP obtained in this way had a zero-net charge. During the MD simulations, the atomic positions of Y and F atoms were maintained fixed at their initial values, avoiding the need of considering explicitly the interaction between yttrium and fluorine. The interaction of yttrium and fluorine atoms with all other atoms of the system (atoms from water or the ions) was modeled with the CHARMM force-field with electrostatic interactions (due to particle charges) and Lennard-Jones interactions. The Lennard-Jones parameters employed for fluorine were standard CHARMM values. For yttrium, CHARMM does not provide standard values for Lennard-Jones parameters, so we had to derive appropriate values. To this end, we have considered a previous work[51] in which the force field for yttrium and in particular for yttrium−oxygen interactions was studied and modeled using a Buckingham potential. We converted the Buckingham potential parameters considered in that work to parameters for a Lennard-Jones potential. We have found a good agreement between the two potentials (Buckingham potential employed by Busker et al.[51] and the Lennard-Jones potential employed in CHARMM) by assigning the following Lennard-Jones parameters to yttrium $R_{min} = 0.3420$ nm and $\varepsilon = -0.001298$ kcal/mol. All MD simulations were performed using the NAMD program, version 1.9.[52] For all technical details of MD simulations, see Supporting Information.

## ■ ASSOCIATED CONTENT

### Supporting Information

The Supporting Information is available free of charge on the ACS Publications website at DOI: 10.1021/jacs.7b09821.

Further information on particles characterization; electrokinetic measurements; temperature, cation and anion roles, and the effect of free ions and washing process of NPs; IR spectroscopy study; XPS results; more cases of citrate bridges in other NPs; methods for MD simulations (PDF)

movie of the spontaneous formation of citrate bridge (ZIP)

## ■ AUTHOR INFORMATION


### Corresponding Authors

*jfaraudo@icmab.es (MD simulations)
*ramon.yanez@uab.cat (experimental)

### ORCID

Jordi Martínez-Esaín: 0000-0002-8420-8559
Jordi Faraudo: 0000-0002-6315-4993
Susagna Ricart: 0000-0003-4196-2081


### Notes

The authors declare no competing financial interest.

## ■ ACKNOWLEDGMENTS

This work was supported by Spanish Ministry of Economy and Competitiveness through the "Severo Ochoa" Programme for Centres of Excellence in R&D (SEV-2015-0496), CONSOLIDER Excellence Network (MAT2015-68994-REDC), COACHSUPENERGY project (MAT2014-51778-C2-1-R, cofinanced by the European Regional Development Fund) and SUPERINKS project (RTC-2015-3640-3, cofinanced by the European Regional Development Fund). We also thank support from the European Union for EUROTAPES project (FP7-NMP-Large-2011-280432) and ULTRASUPERTAPE project (H2020 ERC-2014-ADG-669504) and from the Catalan Government with 2014-SGR-753 and Xarmae. The authors acknowledge the technical support of Servei de Microscòpia, NMR Service and Servei de Difracció de Raigs-X, all at the UAB, to the Soft Materials Service and Dr. Judit Oró (Microscope Service) at the ICMAB-CSIC, Dr. Guillaume Sauthier for his support in XPS analysis, and Dr. Eduardo Solano for his scientific discussions. J.M.E. acknowledges the PIF predoctoral fellowship from the Universitat Autònoma de Barcelona. J.F. thanks CESGA Supercomputing Center for technical support and the use of computational resources. We thank Justin J. Charette for help with English usage.

## ■ REFERENCES


(1) Fischer, S.; Bronstein, N. D.; Swabeck, J. K.; Chan, E. M.; Alivisatos, A. P. *Nano Lett.* **2016**, *16*, 7241.
(2) Ingham, B.; Lim, T. H.; Dotzler, C. J.; Henning, A.; Toney, M. F.; Tilley, R. D. *Chem. Mater.* **2011**, *23*, 3312.
(3) Thanh, N. T. K.; Maclean, N.; Mahiddine, S. *Chem. Rev.* **2014**, *114*, 7610.
(4) Abbas, M.; Zou, Q.; Li, S.; Yan, X. *Adv. Mater.* **2017**, *29*, 1605021.
(5) Ramin, M. A.; Sindhu, K. R.; Appavoo, A.; Oumzil, K.; Grinstaff, M. W.; Chassande, O.; Barthélémy, P. *Adv. Mater.* **2017**, *29*, 1605227.
(6) Abdukayum, A.; Chen, J. T.; Zhao, Q.; Yan, X. P. *J. Am. Chem. Soc.* **2013**, *135*, 14125.
(7) Gonzalez-Carter, D. A.; Leo, B. F.; Ruenraroengsak, P.; Chen, S.; Goode, A. E.; Theodorou, I. G.; Chung, K. F.; Carzaniga, R.; Shaffer, M. S. P.; Dexter, D. T.; Ryan, M. P.; Porter, A. E. *Sci. Rep.* **2017**, *7*, 42871.
(8) Tian, Z. R.; Voigt, J. a; Liu, J.; McKenzie, B.; McDermott, M. J.; Rodriguez, M. a; Konishi, H.; Xu, H. *Nat. Mater.* **2003**, *2*, 821.
(9) Cantarutti, C.; Raimondi, S.; Brancolini, G.; Corazza, A.; Giorgetti, S.; Ballico, M.; Zanini, S.; Palmisano, G.; Bertoncin, P.; Marchese, L.; Patrizia Mangione, P.; Bellotti, V.; Corni, S.; Fogolari, F.; Esposito, G. *Nanoscale* **2017**, *9*, 3941.
(10) Moise, S.; Céspedes, E.; Soukup, D.; Byrne, J. M.; El Haj, A. J.; Telling, N. D. *Sci. Rep.* **2017**, *7*, 39922.



DOI: 10.1021/jacs.7b09821
J. Am. Chem. Soc. 2018, 140, 2127−2134

(11) Peng, H. Y.; Ding, B. B.; Ma, Y. C.; Sun, S. Q.; Tao, W.; Guo, Y. C.; Guo, H. C.; Yang, X. Z.; Qian, H. S. *Appl. Surf. Sci.* **2015**, *357*, 2408.
(12) Ruggiero, E.; Alonso-de Castro, S.; Habtemariam, A.; Salassa, L. *Dalt. Trans.* **2016**, *45*, 13012.
(13) Xiong, L.; Shen, B.; Behera, D.; Gambhir, S. S.; Chin, F. T.; Rao, J. *Nanoscale* **2013**, *5*, 3253.
(14) Li, X.; Gai, S.; Li, C.; Wang, D.; Niu, N.; He, F.; Yang, P. *Inorg. Chem.* **2012**, *51*, 3963.
(15) Gai, S.; Li, C.; Yang, P.; Lin, J. *Chem. Rev.* **2014**, *114*, 2343.
(16) Paik, T.; Chacko, A.-M.; Mikitsh, J. L.; Friedberg, J. S.; Pryma, D. A.; Murray, C. B. *ACS Nano* **2015**, *9*, 8718.
(17) Zhang, Z.; Ma, X.; Geng, Z.; Wang, K.; Wang, Z. *RSC Adv.* **2015**, *5*, 33999.
(18) Ai, F.; Sun, T.; Xu, Z.; Wang, Z.; Kong, W.; To, M. W.; Wang, F.; Zhu, G. *Dalt. Trans.* **2016**, *45*, 13052.
(19) Al-Johani, H.; Abou-Hamad, E.; Jedidi, A.; Widdifield, C. M.; Viger-Gravel, J.; Sangaru, S. S.; Gajan, D.; Anjum, D. H.; Ould-Chikh, S.; Hedhili, M. N.; Gurinov, A.; Kelly, M. J.; El Eter, M.; Cavallo, L.; Emsley, L.; Basset, J.-M. *Nat. Chem.* **2017**, *9*, 890.
(20) Boles, M. A.; Ling, D.; Hyeon, T.; Talapin, D. V. *Nat. Mater.* **2016**, *15*, 141.
(21) De Roo, J.; Justo, Y.; De Keukeleere, K.; Van den Broeck, F.; Martins, J. C.; Van Driessche, I.; Hens, Z. *Angew. Chem., Int. Ed.* **2015**, *54*, 6488.
(22) Yang, M.; Chan, H.; Zhao, G.; Bahng, J. H.; Zhang, P.; Král, P.; Kotov, N. a. *Nat. Chem.* **2017**, *9*, 287.
(23) Salorinne, K.; Malola, S.; Wong, O. A.; Rithner, C. D.; Chen, X.; Ackerson, C. J. *Nat. Commun.* **2016**, *7*, 10401.
(24) Ye, X.; Chen, J.; Engel, M.; Millan, J. A.; Li, W.; Qi, L.; Xing, G.; Collins, J. E.; Kagan, C. R.; Li, J.; Glotzer, S. C.; Murray, C. B. *Nat. Chem.* **2013**, *5* (6), 466.
(25) Nie, Z.; Petukhova, A.; Kumacheva, E. *Nat. Nanotechnol.* **2010**, *5*, 15.
(26) Murray, C. B.; Kagan, C. R.; Bawendi, M. G. *Annu. Rev. Mater. Sci.* **2000**, *30*, 545.
(27) Shevchenko, E. V.; Talapin, D. V.; Kotov, N. A.; O'Brien, S.; Murray, C. B. *Nature* **2006**, *439*, 55.
(28) Wang, X.; Zhuang, J.; Peng, Q.; Li, Y. *Nature* **2005**, *437*, 121.
(29) Bobtelsky, M.; Graus, B. *J. Am. Chem. Soc.* **1955**, *77*, 1990.
(30) Holzwarth, U.; Gibson, N. *Nat. Nanotechnol.* **2011**, *6*, 534.
(31) Kim, D. M.; Lee, S. H.; Alexander, W. B.; Kim, K. B.; Oh, Y. S.; Lee, S. M. *J. Am. Ceram. Soc.* **2011**, *94*, 3455.
(32) Maślankiewicz, P.; Szade, J.; Winiarski, A.; Daniel, P. *Cryst. Res. Technol.* **2005**, *40*, 410.
(33) Moulder, J. F.; Stickle, W. F.; Sobol, P. E.; Bomben, K. D. *Handbook of X-ray Photoelectron Spectroscopy*; Perkin-Elmer Corporation: Waltham, 1992.
(34) Frenkel, D.; Smit, B. *Understanding Molecular Simulation*; Academic Press: San Diego, 2002.
(35) Zherebetskyy, D.; Scheele, M.; Zhang, Y.; Bronstein, N.; Thompson, C.; Britt, D.; Salmeron, M.; Alivisatos, P.; Wang, Lin-Wang *Science* **2014**, *344*, 1380.
(36) Anderson, N. C.; Hendricks, M. P.; Choi, J. J.; Owen, J. S. *J. Am. Chem. Soc.* **2013**, *135*, 18536.
(37) Humphrey, W.; Dalke, A.; Schulten, K. *J. Mol. Graphics* **1996**, *14*, 33.
(38) Hénin, J.; Fiorin, G.; Chipot, C.; Klein, M. L. *J. Chem. Theory Comput.* **2010**, *6*, 35.
(39) Calero, C.; Faraudo, J.; Bastos-González, D. *J. Am. Chem. Soc.* **2011**, *133*, 15025.
(40) Martinez-Esain, J.; Ros, J.; Ricart, S.; Faraudo, J.; Yáñez, R.; Submitted to Langmuir, **2018**.
(41) Zhang, T.; Brown, J.; Oakley, R. J.; Faul, C. F. J. *Curr. Opin. Colloid Interface Sci.* **2009**, *14*, 62.
(42) Shen, J.; Xin, X.; Liu, T.; Wang, S.; Yang, Y.; Luan, X.; Xu, G.; Yuan, S. *Langmuir* **2016**, *32*, 9548.
(43) Faraudo, J.; Martin-Molina, A. *Curr. Opin. Colloid Interface Sci.* **2013**, *18*, 517.
(44) Liang, H.; Harries, D.; Wong, G. C. L. *Proc. Natl. Acad. Sci. U. S. A.* **2005**, *102*, 11173.
(45) Min, Y.; Akbulut, M.; Kristiansen, K.; Golan, Y.; Israelachvili, J. *Nat. Mater.* **2008**, *7*, 527.
(46) Mackerell, A. D.; Feig, M.; Brooks, C. L. *J. Comput. Chem.* **2004**, *25*, 1400.
(47) MacKerell, A. D.; Bashford, D.; Dunbrack, R. L.; Evanseck, J. D.; Field, M. J.; Fischer, S.; Gao, J.; Guo, H.; Ha, S.; Joseph-McCarthy, D.; Kuchnir, L.; Kuczera, K.; Lau, F. T. K.; Mattos, C.; Michnick, S.; Ngo, T.; Nguyen, D. T.; Prodhom, B.; Reiher, W. E.; Roux, B.; Schlenkrich, M.; Smith, J. C.; Stote, R.; Straub, J.; Watanabe, M.; Wiórkiewicz-Kuczera, J.; Yin, D.; Karplus, M.; Dunbrack, R. L.; Evanseck, J. D.; Field, M. J.; Fischer, S.; Gao, J.; Guo, H.; Ha, S.; Joseph-McCarthy, D.; Kuchnir, L.; Kuczera, K.; Lau, F. T. K.; Mattos, C.; Michnick, S.; Ngo, T.; Nguyen, D. T.; Prodhom, B.; Reiher, W. E.; Roux, B.; Schlenkrich, M.; Smith, J. C.; Stote, R.; Straub, J.; Watanabe, M.; Wiórkiewicz-Kuczera, J.; Yin, D.; Karplus, M. *J. Phys. Chem. B* **1998**, *102*, 3586.
(48) Vanommeslaeghe, K.; Hatcher, E.; Acharya, C.; Kundu, S.; Zhong, S.; Shim, J. E.; Darian, E.; Guvench, O.; Lopes, P.; Vorobyov, I.; MacKerell, J. A. D. *J. Comput. Chem.* **2009**, *31*, 671.
(49) Bernal, S.; Botana, F. J.; Calvino, J. J.; López, C.; Pérez-Omil, J. a.; Rodríguez-Izquierdo, J. M. *J. Chem. Soc., Faraday Trans.* **1996**, *92*, 2799.
(50) Bernal, S.; Botana, F. J.; Calvino, J. J.; López-Cartes, C.; Pérez-Omil, J. A.; Rodríguez-Izquierdo, J. M. *Ultramicroscopy* **1998**, *72*, 135.
(51) Busker, G.; Chroneos, A.; Grimes, R. W.; Chen, I.-W. *J. Am. Ceram. Soc.* **1999**, *82*, 1553.
(52) Phillips, J. C.; Braun, R.; Wang, W.; Gumbart, J.; Tajkhorshid, E.; Villa, E.; Chipot, C.; Skeel, R. D.; Kalé, L.; Schulten, K. *J. Comput. Chem.* **2005**, *26*, 1781−1802.


DOI: 10.1021/jacs.7b09821
*J. Am. Chem. Soc.* 2018, 140, 2127−2134